Supramolecular Organization and Dual Function of the IsiA Chlorophyll-Binding Protein in Cyanobacteria†

Nataliya Yeremenko,‡,§ Roman Kouřil,§,|| Janne A. Ihalainen,⊥ Sandrine D'Haene,⊥ Niels van Oosterwijk,|| Elena G. Andrizhiyevskaya,⊥ Wilko Keegstra,|| Henk L. Dekker,@ Martin Hagemann,# Egbert J. Boekema,|| Hans C. P. Matthijs,‡ and Jan P. Dekker*,⊥

Aquatic Microbiology, Institute of Biodiversity and Ecosystem Dynamics, Faculty of Science, Universiteit van Amsterdam, Nieuwe Achtergracht 127, 1018 WS Amsterdam, The Netherlands, Department of Biophysical Chemistry, Groningen Biomolecular Sciences and Biotechnology Institute, University of Groningen, Nijenborgh 4, 9747 AG Groningen, The Netherlands, Division of Physics and Astronomy, Faculty of Sciences, Vrije Universiteit, De Boelelaan 1081, 1081 HV Amsterdam, The Netherlands, Mass Spectrometry Group, Swammerdam Institute for Life Sciences, University of Amsterdam, Nieuwe Achtergracht 166, 1018 WV Amsterdam, The Netherlands, and Fachbereich Biowissenschaften, Pflanzenphysiologie, Universität Rostock, Albert-Einstein-Strasse 3a, 18051 Rostock, Germany

Received June 14, 2004; Revised Manuscript Received July 6, 2004

ABSTRACT: A significant part of global primary productivity is provided by cyanobacteria, which are abundant in most marine and freshwater habitats. In many oceanographic regions, however, the concentration of iron can be so low that it limits growth. Cyanobacteria respond to this condition by expressing a number of iron stress inducible genes, of which the *isiA* gene encodes a chlorophyll-binding protein known as IsiA or CP43′. It was recently shown that 18 IsiA proteins encircle trimeric photosystem I (PSI) under iron-deficient growth conditions. We report here that after prolonged growth of *Synechocystis* PCC 6803 in an iron-deficient medium, the number of bound IsiA proteins can be much higher than previously known. The largest complexes bind 12−14 units in an inner ring and 19−21 units in an outer ring around a PSI monomer. Fluorescence excitation spectra indicate an efficient light harvesting function for all PSI-bound chlorophylls. We also find that IsiA accumulates in cyanobacteria in excess of what is needed for functional light harvesting by PSI, and that a significant part of IsiA builds supercomplexes without PSI. Because the further decline of PSI makes photosystem II (PSII) increasingly vulnerable to photooxidation, we postulate that the surplus synthesis of IsiA shields PSII from excess light. We suggest that IsiA plays a surprisingly versatile role in cyanobacteria, by significantly enhancing the light harvesting ability of PSI and providing photoprotection for PSII.

Iron is one of the most abundant elements on Earth. However, the share actually available for living organisms in oxygen-rich aquatic environments is limited. This is especially true in the oceans, where bioproductivity is limited by the low solubility of the iron(III) ion in slightly alkaline water (*1*−*4*). The ubiquitous cyanobacteria that make an important contribution to global bioproductivity adapt well to a deficiency of iron (*3*, *5*). The lack of iron and the adaptation at large concern the photosynthetic properties of these organisms (*6*).

The role of iron in oxygenic photosynthesis is obvious from the obligatory role of three iron−sulfur clusters in electron transport in photosystem I (PSI)[1] (*7*, *8*). It is therefore no surprise that iron limitation stress affects primarily PSI. Under iron-deficient conditions, the content of PSI decreases substantially more than that of PSII (*9*, *10*). Nevertheless, growth continues despite the lack of iron, and only after extended periods of time in which the iron content per cell is lowered to its minimum is a stationary phase reached. For cells to keep growing, a gradual adaptation must help overcome the increasingly heavy burden of shortage of iron. A major and well-documented adaptation response is the induction of the iron (limitation) stress inducible *isiAB* operon (*6*). This operon expresses two proteins, IsiA and IsiB. IsiB, flavodoxin, has a clear function in iron limitation stress; it replaces the iron-rich soluble electron transfer

† R.K. and J.A.I. were supported by the European Union (Grant HPRN-CT-2002-00248). The work of J.P.D. and E.J.B. was supported by a grant from the Foundation of Life and Earth Sciences (ALW) of NWO. The Q-TOF mass spectrometer was largely funded by grants from the Council for Medical Sciences and the nano HPLC by a grant from the Council for Chemical Sciences of The Netherlands Organization for Scientific Research (NWO).

* To whom correspondence should be addressed. Telephone: +31 20 4447931. Fax: +31 20 4447999. E-mail: JP.Dekker@few.vu.nl.

‡ Institute of Biodiversity and Ecosystem Dynamics, Faculty of Science, Universiteit van Amsterdam.

§ These authors contributed equally to this work.

|| University of Groningen.

⊥ Vrije Universiteit.

@ Swammerdam Institute for Life Sciences, University of Amsterdam.

Universität Rostock.

[1] Abbreviations: β-DM, *n*-dodecyl β-D-maltoside; fwhm, full width at half-maximum; Isi, iron stress inducible; MSA, multivariate statistical analysis; Pcb, prochlorophyte chlorophyll *a*/*b*; PSI, photosystem I; PSII, photosystem II.

10.1021/bi048772l CCC: $27.50
Published on Web 07/23/2004

protein ferredoxin (*9*). The chlorophyll-binding protein IsiA is even more strongly induced than its dicistronic partner IsiB, but its function and cellular localization have been a puzzling topic for a considerable period of time (*6*, *11*). The surprise about the functional role of IsiA came a few years ago when a large complex of a PSI trimer encircled by 18 monomers of IsiA was revealed by electron microscopy (*12*, *13*).

The IsiA protein belongs to the so-called core complex antenna family of chlorophyll-binding proteins, a family of proteins that is more widespread and important than was realized until only a few years ago (*11*). Its most well-known members are the CP47 and CP43 core antenna proteins of photosystem II (PSII), which are structurally resolved down to 3.5 Å resolution (*14*). CP47 and CP43 are located at fixed positions in the PSII supercomplex and mediate the transfer of excitation energy from the peripheral antenna to the photochemical reaction center of PSII (*15*). Other members of the core complex antenna family are the prochlorophyte chlorophyll *a*/*b* (Pcb) proteins, whose sequences are homologous with that of CP43 (*11*). It was shown that Pcb proteins from *Prochloron didemni* (*16*) and a moderate-light-adapted *Prochlorococcus* strain (*17*) can bind to dimeric PSII, whereas other Pcb proteins from the latter species and from an extremely low-light-adapted *Prochlorococcus* species form a ring of 18 units around trimeric PSI (*17*, *18*), giving rise to a supercomplex with an overall structure very similar to that of the $(PSI)_3(IsiA)_{18}$ supercomplex of cyanobacteria.

Spectroscopic evidence has indicated that IsiA provides an additional light harvesting function (*19*, *20*), and thus, its function is explained by the supply of more light to the gradually shrinking pool of active PSI centers. In the 18-ring structure, the light harvesting capacity of the PSI trimer is approximately doubled compared to that of the PSI core complex (*20*, *21*).

The pronounced induction of IsiA has given rise to proposals for two additional roles in cell physiology, i.e., to protect PSII against oxidative stress by shading it (*10*, *22*) and as a store for chlorophyll to enable its rapid addition to newly synthesized PSI formed after the iron content in the growth environment increases (*6*). The importance of protection of PSII against oxidative stress in cyanobacteria deficient in iron has also been confirmed with other observations, such as the induction of the iron stress gene *idiA* (*23*), the downregulation of light harvesting by the phycobilisome antennae of PSII (*24*), and the regulation of expression of a range of PSII and PSI genes from gene array analysis (*25*). Evidence that oxidative stress rather than the lack of iron triggers the induction of the *isiAB* operon has also been presented (*23*, *26*).

Here we describe how iron limitation stress during extended periods of time gives rise to abundant synthesis of the IsiA protein in complexes that show highly variable stoichiometries of PSI and IsiA. We characterize this as an optimal adaptation to the degree of iron limitation stress for flexible light harvesting. In addition to the antenna function of IsiA complexes associated with PSI, free IsiA supercomplexes without associated PSI may contribute to the shading of PSII for prevention of oxidative stress.

MATERIALS AND METHODS

Organism and Culture. Wild-type *Synechocystis* sp. PCC 6803 and the *psaFJ*$^-$ mutant (*26*) were grown at 30 °C in liquid BG11 medium at a light intensity of 50 μmol of photons m^{-2} s^{-1} in ambient air. Iron deficiency was achieved by omitting all iron sources from the medium. Inoculation for iron-depleted culture was by 20−30-fold dilution of cells (washed three times) that were pregrown in normal medium. In the work presented here, cells harvested 2−23 days after inoculation were used.

Cell Fractionation. Cells were broken and thylakoid membranes isolated as described previously (*27*). Freshly isolated thylakoid membranes (0.15 mg of chlorophyll *a*/mL) were solubilized with 0.5% (w/v) *n*-dodecyl β-D-maltoside (β-DM) and centrifuged at 9000*g* for 3 min. The supernatant was filtered on a Titan PVDF syringe filter (0.45 μm) and subjected to size exclusion chromatography as described previously (*28*), using a Superdex 200 HR 10/30 column (Pharmacia), a running buffer consisting of 20 mM Bis-Tris (pH 6.5), 5 mM $MgCl_2$, and 0.03% β-DM, and an on-line diode array detector (Shimadzu SPD-M10A). Fractions containing particles with sizes of supercomplexes were used for further analysis.

SDS−PAGE and Mass Spectrometry. FPLC fractions were concentrated on a Microcon YM-10 membrane (Millipore), and the protein content was estimated by the assay according to Bradford (Bio-Rad). The protein composition was analyzed by Tris-Tricine SDS−PAGE (*29*). Protein bands were cut out off the gel, reduced with DTT, S-alkylated with iodoacetamide, and digested with trypsin (sequence-grade, Roche, Basel, Switzerland) as described previously (*30*). The digested peptide mixture was loaded onto the precolumn of an Ultimate nano-HPLC system (LC Packings, Amsterdam, The Netherlands) and separated on a PepMap C18 nano reversed phase column (75 μm inside diameter). Elution was performed using a gradient of 5 to 40% acetonitrile with 0.1% formic acid. The flow was infused directly into an ESI-QTOF mass spectrometer (Micromass) via a modified nano-electrospray device (New Objective, Woburn, MA). MS/MS (tandem mass spectrometry) experiments were conducted with argon as the collision gas at a pressure of 4×10^{-5} bar measured on the quadruple pressure gauge. The acquired peptide MSMS spectra were used in a search of the SwissProt database.

Spectroscopy. For 5 K absorption and fluorescence measurements, the samples were diluted in a buffer containing 20 mM Bis-Tris (pH 6.5), 10 mM $MgCl_2$, 10 mM $CaCl_2$, 0.02% β-DM, and 66% (w/w) glycerol. The ODs of the samples used for fluorescence and absorbance measurements were ~0.1 and ~0.6 cm^{-1}, respectively, at the Q_y absorption maximum. Low-temperature absorption was assessed on a home-built spectrophotometer. Fluorescence emission spectra were recorded on a home-built spectrograph CCD fluorimeter, using an excitation wavelength of 420 nm. Fluorescence excitation spectra were recorded on a home-built spectrometer with emission wavelengths of 722 and 742 nm (fwhm of 5 nm).

Electron Microscopy. EM was performed as described in ref *28*. Briefly, EM specimens were prepared on glow-discharged carbon-coated grids, using 2% uranyl acetate as a negative stain. EM was performed on a Philips FEG20

electron microscope. Semiautomated data acquisition was used to record a total of 7500 images (2048 × 2048 pixels) at a magnification of 66850× with a Gatan 4000 SP 4K slow-scan CCD camera. The step size (after the binning) was 30 μm, corresponding to a pixel size of 4.5 Å at the specimen level, and projections were selected for single-particle averaging (*31*) with Groningen Image Processing software. Projections were aligned by multireference alignment, and aligned images were subjected to multivariate statistical analysis (MSA). After MSA, particles were classified and summed and class sums were used in a next cycle of multi-reference alignment, MSA, and classification. Final sums within homogeneous classes were obtained by reference-free alignment procedures (*32*).

RESULTS

Accumulation and Structural Diversity of PSI−IsiA Supercomplexes. To investigate the relation among the number of bound IsiA units in PSI−IsiA supercomplexes, the monomeric or trimeric aggregation state of PSI (*33*), and the degree of iron starvation, we analyzed these complexes at various times after the start of a culture in an iron-free medium. We prepared supercomplexes by a short incubation with the nonionic detergent β-DM, separated these complexes by gel filtration chromatography as described previously (*28*, *34*), and investigated the freshly prepared supercomplexes by electron microscopy and image analysis. Because initial experiments indicated that many different types of supercomplexes occur during the various stages of iron deficiency, we analyzed a very large set of single-particle projections, to obtain a statistically satisfactory set of projections. A total number of 7500 images were processed, from which nearly 60 000 single-particle projections could be selected.

Figure 1 shows that besides the "standard" $(PSI)_3(IsiA)_{18}$ complex (Figure 1a) various other ring-shaped complexes can also be discerned, with both smaller and larger contents of IsiA, in particular under conditions of prolonged iron limitation. Relatively well-resolved are ringlike structures without a central mass. The largest complex is an almost circularly shaped double-ring structure (Figure 1i) that consists of inner and outer rings of 14 and 21 units, respectively. Slightly smaller and oval-shaped complexes consisting of 13 and 20 (Figure 1h) and of 12 and 19 units (Figure 1g) were also detected in significant numbers. Single rings of 12 and 13 units with a size similar to those of the inner rings of the double rings (Figure 1b,c), as well as partial double and single rings of variable sizes (see Figure 1o for an example), were observed as well.

Many other complexes, however, do contain a central complex resembling monomeric or trimeric PSI. After a few days of culture in an iron-free medium, a $(PSI)_3(IsiA)_7$ complex is abundant (Figure 1d), whereas after ~20 days of culture, single and double closed rings of IsiA around a particle with the size and shape of monomeric PSI can be detected in significant numbers (Figure 1e,f,j−l). The central mass of the best-resolved complex (Figure 1e) exhibits the typical features of PSI. In the largest complex (Figure 1l), stain accumulation in the center of the complex suggests that the inner ring of 14 units (Figure 1n) is too large for the central complex, which is expected if a ring of 12 units is just large enough to encircle monomeric PSI (Figure 1e).

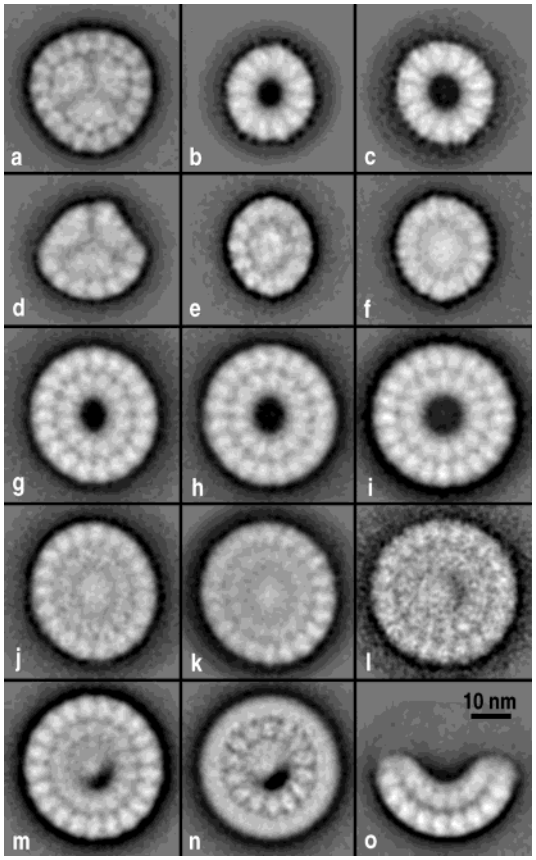

FIGURE 1: Processed top views of PSI−IsiA and IsiA supercomplexes obtained by electron microscopy. (a−c and e−o) Results of statistical analysis and classification of 59 000 particles from wild-type *Synechocystis* PCC 6803. A total of 47 000 projections could be assigned to specific complexes. Closed rings of IsiA consist of 12, 13, or 18 copies in a single ring (b, c, and a, respectively) along with 19, 20, and 21 copies in a second ring surrounding 12, 13, and 14 copies in an inner ring (g−i). The center of the complexes can be occupied by a either a PSI trimer (a) or a monomer (e, f, and j−l). The relative abundance of these complexes was ~19% (a), ~8% (b), ~16% (c), ~9% (e), ~19% (f), ~4% (g), ~5% (h), ~1% (i), ~4% (j), ~6% (k), ~5% (l), and ~4% (o). The images of panels m and n contain a larger number of projections than image l but have the same number of 14 + 21 IsiA copies. Since individual projections have been aligned in different ways, they show fuzziness in either the inner or outer ring, caused by rotational flexibility between these rings (see the text for details). (d) Results of analysis of 6000 particles from a *Synechocystis psaFJ*$^-$ mutant (see ref *28*). A specific complex of trimeric PSI with seven IsiA proteins attached (d) was observed in this set. In addition, this set yielded PSI trimers with a closed ring of 17 units (*28*) and rings and partial rings similar to panels b and c and o, respectively.

The shapes and sizes of the rings with a central complex appear to be very similar to the shapes and sizes of those without.

We noticed that relatively little detail is resolved in the projection maps of Figure 1j−l, despite the large number of processed projections. For complexes with 14 + 21 IsiA copies, the monomer has the expected shape, but only in classes with small numbers of projections summed (Figure 1l). With an increase in the number of summed projections, the features of the outer ring improve, but the monomer and the inner ring do not improve substantially (Figure 1m). The features of the inner ring of the projection map of Figure 1m could be improved by masking the outer ring of the individual projections during an additional alignment step, but at the cost of detail in the outer ring (Figure 1n). This

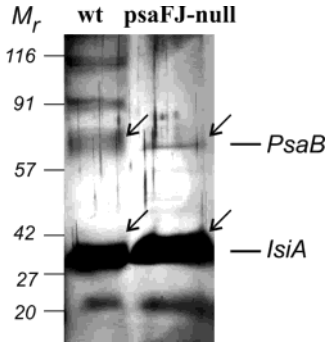

FIGURE 2: Silver-stained SDS−PAGE of proteins of fractions from WT and *psaFJ*$^-$ mutant cells grown in iron-deficient media. Arrows show the bands analyzed by mass spectrometry.

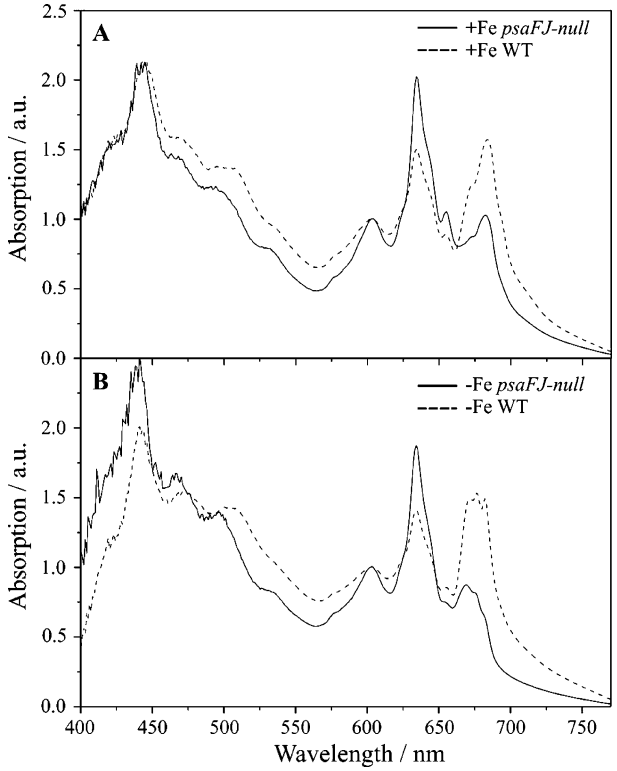

FIGURE 3: Absorption spectra monitored at 5 K of WT and *psaFJ*$^-$ mutant cells grown in iron-replete medium (A) or for 5 days in iron-depleted medium (B).

demonstrates that the fuzziness in Figure 1l,m is caused by rotational flexibility between both rings. The fact that the outer ring has seven more copies of IsiA than the inner ring explains why it becomes overall better aligned in Figure 1m. Further analysis showed that the rotational flexibility between both rings in this subset of particles appeared to be ∼2−3°, on average.

Molecular Composition of Isolated Supercomplexes. To verify that the supercomplexes depicted in Figure 1 consist of IsiA and PSI, we analyzed the supercomplex-containing fractions from cells grown for ∼20 days in an iron-deficient medium by SDS−PAGE (Figure 2), and subjected the main bands to a mass spectrometry analysis. The lower main bands revealed peptide fragmentation spectra consistent with IsiA, while the upper band revealed peptide fragmentation spectra consistent with PsaB, a core subunit of PSI. These data confirm that IsiA and PSI are the main constituents of supercomplexes from iron-depleted wild-type cells, and that

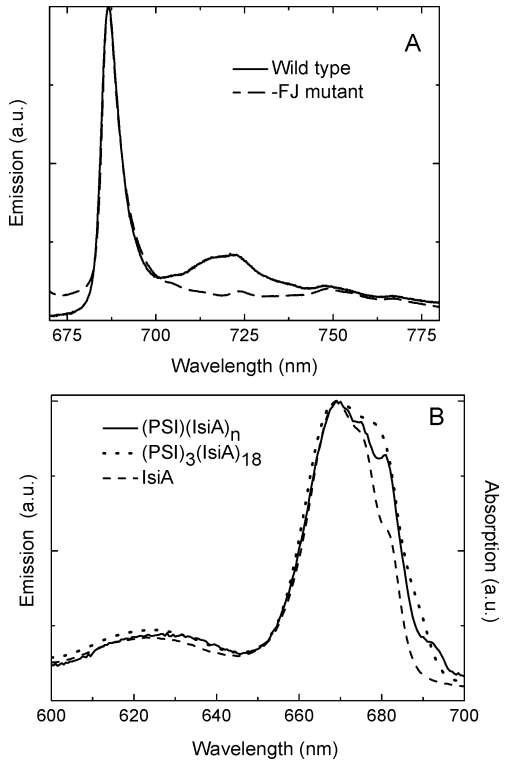

FIGURE 4: Fluorescence emission and excitation spectra (5 K). (A) Fluorescence emission spectra of a fraction from WT cells (—) and from *psaFJ*$^-$ mutant cells (− − −) grown in iron-deficient medium. (B) Fluorescence excitation spectrum (—) of fluorescence detected at 722 nm of a fraction from WT cells grown in iron-deficient medium. The free IsiA contribution (20% at 722 nm; see panel A) has been subtracted from the excitation spectrum. The excitation spectrum of free IsiA was obtained by taking the difference of spectra detected at 742 and 722 nm. The 77 K absorption spectra of the IsiA fraction from the *psaFJ*$^-$ mutant grown in iron-deficient medium (− − −) and the 5 K absorption spectrum from isolated $(PSI)_3(IsiA)_{18}$ particles (···) are shown for comparison.

IsiA alone is the main constituent of the supercomplexes found in the PsaFJ$^-$ mutant.

Spectroscopic Analyses. In iron-replete medium, the growth rates of wild-type (WT) and PsaFJ$^-$ mutant cells are similar. Differences between both strains are visible in the 5 K absorption spectra (Figure 3A). The mutant features a high phycobilisome (628 nm peak) content relative to the assembly of peaks in the 670−690 nm area that represent the chlorophyll proteins of PSI, PSII, and, if present, IsiA. Under iron-depleted conditions, the WT shows a broader 670−690 nm domain, largely due to added absorption at 670 nm caused by IsiA (*19*). The mutant also features this addition, but shifted to the blue due to a decrease in the magnitude of the original peak in the iron-replete spectrum at 680 nm (Figure 3B), indicating a decrease in PSI content.

We recorded 5 K fluorescence emission spectra of the fraction from wild-type cells analyzed in Figure 1 to further confirm the nature of the investigated pigment−protein complexes. The broad band peaking at ∼720 nm shown in Figure 4A can be attributed to PSI (*35*). The fact that this peak is almost absent in iron-stressed mutant cells is consistent with the SDS−PAGE results (Figure 2). The region between 685 and 695 nm represents emission from PSII, which in the PSII core complex of *Synechocystis* 6803 at 5 K consists of a broad band peaking at 688 nm and has a fwhm of 14 nm (E. G. Andrizhiyevskaya, unpublished

observations). The fluorescence spectrum from iron-starved mutant cells is dominated by a band peaking at 686−687 nm but with a fwhm of only 6 nm, which therefore cannot arise from PSII and in fact must arise from IsiA aggregates. IsiA is abundant in the iron-starved mutant cells (Figure 2), and IsiA monomers exhibit a blue-shifted 5 K emission maximum at 682 nm (*19*). The 686 nm emission in wild-type cells must in large part arise from PSI-less IsiA aggregates, because in isolated PSI−IsiA supercomplexes only a very small 686−687 nm emission band is observed (*19*).

We recorded 5 K excitation spectra of the fraction analyzed in Figure 4A to determine whether the IsiA proteins in these IsiA-rich complexes transfer excitation energy to PSI. We analyzed the relative difference in fluorescence detected at 722 and 742 nm to correct for the contributions from free IsiA complexes. The ratios of the contributions of 670 nm states in the absorption spectra belonging to IsiA (*19*) have been compared to those of 681 nm states belonging to PSI. For the absorption spectrum of the $(PSI)_3(IsiA)_{18}$ complex, this ratio was established earlier as 1/0.95 (Figure 4B, dotted line), and for the IsiA aggregates, this ratio is 1/0.5 (Figure 4B, dashed line). For the WT PSI−IsiA fraction analyzed in Figure 1, we determined a ratio in the excitation spectrum of 1/0.81 (Figure 4B, solid line). From these data, we calculated an average number of 10 functionally bound IsiA complexes per PSI monomer, which represents an appreciably stronger light harvesting ability in the "average" PSI−IsiA complex generated by long-term iron limitation compared to the number of six for the "standard" $(PSI)_3(IsiA)_{18}$ complex that occurs predominantly after shorter periods of iron limitation.

DISCUSSION

The original discovery of 18 IsiA monomers in a ring around PSI as published simultaneously by two different research groups in 2001 (*12*, *13*) set the hallmark for continued curiosity about the conditions for accumulation, the structural appearance, and the function of IsiA in cyanobacteria. The current results indicate that IsiA occurs in two different types of complexes, i.e., in sometimes very large PSI−IsiA supercomplexes and in similarly large PSI-free IsiA-only supercomplexes. Fluorescence spectroscopy suggests that both types of complexes occur as such in the thylakoid membranes. It is very likely that the IsiA present in both types of complexes serves different functions.

A major outcome of this work is that the PSI−IsiA supercomplexes show increasingly larger amounts of bound IsiA proteins with increasing levels of iron starvation. The largest particles seen in this work, with a double-IsiA ring around monomeric PSI, would contain ~35 × 16 (560) chlorophylls, which together with 96 chlorophylls of the PSI core complex (*7*) would give a total number of 656 chlorophylls. PSI particles with such large antenna sizes have not been observed before. Biophysical measurements on the standard $(PSI)_3(IsiA)_{18}$ complexes have made clear that the chlorophylls of the IsiA units within the PSI−IsiA supercomplexes act as very efficient light harvesters (*20*, *21*), and excitation spectra of the average long-time iron-depleted PSI−IsiA complex indicated that the additional IsiA complexes must harvest light efficiently as well. The addition of 560 chlorophylls as in the largest PSI−IsiA supercomplexes would give an almost 7-fold increase in the light harvesting ability of PSI.

The image analysis indicated that the two rings that encircle monomeric PSI have rotational disorder of a few degrees with respect to each other. For the efficiency of excitation energy transfer between the rings and from the rings to PSI, a precise match of the IsiA proteins is probably not necessary, because of very fast and multiple excitation transfer routes from IsiA to PSI (*20*, *21*). The increased antenna size will thus provide compensation for the light need of the lower number of PSI centers compared to PSII under iron stress.

Another major result of this work is that IsiA supercomplexes accumulate in cyanobacteria in excess of what is needed for functional light harvesting by PSI. The increase in the narrow-banded 77 K (*6*, *10*) or 5 K (this work) fluorescence emission at 685−687 nm almost immediately after a shift from iron-sufficient to iron-deficient conditions suggests that PSI-free IsiA aggregates occur even in early stages of iron deficiency. It is likely that the excess synthesis of IsiA serves to protect PSII from photooxidative stress. PSII is very vulnerable to photooxidation in the absence of PSI (*24*), and the large number of free IsiA complexes present after prolonged iron limitation stress can simply remove excess excitation energy from the membranes, thus preventing overexcitation and photodamage of PSII. This is in line with earlier reports that advocated a role for overexpressed IsiA in the protection of PSII against high light (*10*, *23*), so the PSI-less IsiA rings may play a role in shading. Some of the free IsiA supercomplexes may also function in forming complexes of newly synthesized PSI under iron-replete conditions (*6*), but for the closed rings, this seems to be unlikely.

It thus appears that the IsiA protein has evolved optimally from the common ancestor of the core complex antenna family of chlorophyll-binding proteins. It not only lacks the large extrinsic loop that CP43 in PSII needs to assist water oxidation (*6*, *14*), it also very likely contains a few additional "linker" chlorophylls (*19*) that could assist in fast and efficient excitation energy transfer from the outer to the inner IsiA ring and from the inner ring to PSI (*20*, *21*). This situation resembles that in green plant PSI, in which several linker chlorophylls have been detected between the peripheral antenna of LHCI proteins from the unrelated Cab gene family and the PSI complex (*36*); however, most important of all is the ability of the IsiA protein, unlike CP47 and CP43, to form large and flexible supramolecular structures, both with itself and with PSI. In this sense, IsiA can be viewed as the cyanobacterial counterpart of LHCII, the main light-harvesting complex for PSII in green plants (*37*) which forms supramolecular structures with and without PSII (*38*) and thus provides the photosystem with both a large functional antenna and a mechanism for regulating the light need for photosynthesis.

In conclusion, after the onset of iron deficiency, IsiA acts in the first place in adding light harvesting capacity to PSI. Concomitantly, a decrease in the rate of electron flow from PSII is needed to balance the remaining photosynthesis activity. This is accompanied by the appearance of large numbers of IsiA molecules in aggregates without PSI, and a next function of IsiA emerges, shielding PSII against excess

light. This means that, depending on the extent of the prevailing iron limitation stress, IsiA serves at least two functions, by acting both in light harvesting and in the dissipation of light energy.

REFERENCES

1. Martin, J. H., Coale, K. H., Johnson, K. S., Fitzwater, S. E., Gordon, R. M., Tanner, S. J., Hunter, C. N., Elrod, V. A., Nowicki, J. L., Coley, T. L., *et al*. (1994) Testing the iron hypothesis in ecosystems of the equatorial pacific ocean, *Nature 371*, 123−129.
2. De Baar, H. J. W., de Jong, J. T. M., Bakker, D. C. E., Loscher, B. M., Veth, C., Bathmann, U., and Smetacek, V. (1995) Importance of iron for plankton blooms and carbon-dioxide drawdown in the southern ocean, *Nature 373*, 412−415.
3. Falkowski, P. G., Barber, R. T., and Smetacek, V. (1998) Biogeochemical controls and feedbacks on ocean primary production, *Science 281*, 200−206.
4. Behrenfeld, M. J., and Kolber, Z. S. (1999) Widespread iron limitation of phytoplankton in the South Pacific Ocean, *Science 283*, 840−843.
5. Ting, C. S., Rocap, G., King, J., and Chisholm, S. W. (2002) Cyanobacterial photosynthesis in the oceans: the origins and significance of divergent light-harvesting strategies, *Trends Microbiol. 10*, 134−142.
6. Burnap, R. L., Troyan, T., and Sherman, L. A. (1993) The highly abundant chlorophyll-protein of iron-deficient *Synechococcus* sp. PCC 7942 (CP43′) is encoded by the *isiA* gene, *Plant Physiol. 103*, 893−902.
7. Jordan, P., Fromme, P., Witt, H. T., Klukas, O., Saenger, W., and Krauss, N. (2001) Three-dimensional structure of phoyosystem I at 2.5 Å resolution, *Nature 411*, 909−917.
8. Fromme, P., Melkozernov, A., Jordan, P., and Krauss, N. (2003) Structure and function of photosystem I: interaction with its soluble electron carriers and external antenna systems, *FEBS Lett. 555*, 40−44.
9. Falk, S., Samson, G., Bruce, D., Huner, N. P. A., and Laudenbach, D. E. (1995) Functional analysis of the iron-stress induced CP43′ polypeptide of PS II in the cyanobacterium *Synechococcus* sp. PCC 7942, *Photosynth. Res. 45*, 51−60.
10. Sandström, S., Park, Y. I., Öquist, G., and Gustafsson, P. (2001) CP43′, the isiA gene product, functions as an excitation energy dissipator in the cyanobacterium *Synechococcus* sp. PCC 7942, *Photochem. Photobiol. 74*, 431−437.
11. Green, B. R. (2003) The evolution of light-harvesting antennas, in *Light-Harvesting Antennas in Photosynthesis* (Green, B. R., and Parson, W. W., Eds.) pp 129−168, Kluwer Academic Publishers, Dordrecht, The Netherlands.
12. Bibby, T. S., Nield, J., and Barber, J. (2001) Iron deficiency induces the formation of an antenna ring around trimeric photosystem I in cyanobacteria, *Nature 412*, 743−745.
13. Boekema, E. J., Hifney, A., Yakushevska, A. E., Piotrowski, M., Keegstra, W., Berry, S., Michel, K. P., Pistorius, E. K., and Kruip, J. (2001) A giant chlorophyll-protein complex induced by iron-deficiency in cyanobacteria, *Nature 412*, 745−748.
14. Ferreira, K. N., Iverson, T. M., Maghlaoui, K., Barber, J., and Iwata, S. (2004) Architecture of the photosynthetic oxygen-evolving center, *Science 303*, 1831−1838.
15. Van Amerongen, H., and Dekker, J. P. (2003) Light-harvesting in photosystem II, in *Light-Harvesting Antennas in Photosynthesis* (Green, B. R., and Parson, W. W., Eds.) pp 219−251, Kluwer Academic Publishers, Dordrecht, The Netherlands.
16. Bibby, T. S., Nield, J., Chen, M., Larkum, A. W. D., and Barber, J. (2003) Structure of a photosystem II supercomplex isolated from *Prochloron didemni* retaining its chlorophyll *a*/*b* light-harvesting system, *Proc. Natl. Acad. Sci. U.S.A. 100*, 9050−9054.
17. Bibby, T. S., Mary, I., Nield, J., Partensky, F., and Barber, J. (2003) Low-light-adapted *Prochlorococcus* species possess specific antennae for each photosystem, *Nature 424*, 1051−1054.
18. Bibby, T. S., Nield, J., Partensky, F., and Barber, J. (2001) Oxyphotobacteria: Antenna ring around PS1, *Nature 413*, 590.
19. Andrizhiyevskaya, E. G., Schwabe, T. M. E., Germano, M., D'Haene, S., Kruip, J., van Grondelle, R., and Dekker, J. P. (2002) Spectroscopic properties of PSI−IsiA supercomplexes of the cyanobacterium *Synechococcus* PCC 7942, *Biochim. Biophys. Acta 1556*, 265−272.
20. Melkozernov, A. N., Bibby, T. S., Lin, S., Barber, J., and Blankenship, R. E. (2003) Time-resolved absorption and emission show that the CP43′ antenna ring of iron-stressed *Synechocystis* sp. PCC 6803 is efficiently coupled to the photosystem I reaction center core, *Biochemistry 42*, 3893−3903.
21. Andrizhiyevskaya, E. G., Frolov, D., van Grondelle, R., and Dekker, J. P. (2004) Energy transfer and trapping in the photosystem I complex of *Synechococcus* PCC 7942 and in its supercomplex with IsiA, *Biochim. Biophys. Acta 1656*, 104−113.
22. Park, Y. I., Sandström, S., Gustafsson, P., and Öquist, G. (1999) Expression of the *isiA* gene is essential for the survival of the cyanobacterium *Synechococcus* sp PCC7942 by protecting photosystem II from excess light under iron limitation, *Mol. Microbiol. 32*, 123−129.
23. Michel, K. P., and Pistorius, E. K. (2004) Adaptation of the photosynthetic electron transport chain in cyanobacteria to iron deficiency: The function of IdiA and IsiA, *Physiol. Plant. 120*, 36−50.
24. Sandström, S., Ivanov, A. G., Park, Y. I., Öquist, G., and Gustafsson, P. (2002) Iron stress responses in the cyanobacterium *Synechocystis* sp. PCC 7942, *Physiol. Plant. 116*, 255−263.
25. Singh, A. K., McIntyre, L. M., and Sherman, L. A. (2003) Microarray analysis of the genome-wide response to iron deficiency and iron reconstitution in the cyanobacterium *Synechocystis* sp. PCC 6803, *Plant Physiol. 132*, 1825−1839.
26. Jeanjean, R., Zuther, E., Yeremenko, N., Havaux, M., Matthijs, H. C. P., and Hagemann, M. (2003) A photosystem I *psaFJ-null* mutant of the cyanobacterium *Synechocystis* PCC 6803 expresses the *isiAB* operon under iron replete conditions, *FEBS Lett. 549*, 52−56.
27. Scholts, M. J. C., Aardewijn, P., and van Walraven, H. S. (1996) Membrane vesicles from *Synechocystis* 6803 showing proton and electron transport and high ATP synthase activities, *Photosynth. Res. 47*, 301−305.
28. Kouril, R., Yeremenko, N., D'Haene, S., Yakushevska, A. E., Keegstra, W., Matthijs, H. C. P., Dekker, J. P., and Boekema, E. J. (2003) Photosystem I trimers from *Synechocystis* PCC 6803 lacking the PsaF and PsaJ subunits bind an IsiA ring of 17 units, *Biochim. Biophys. Acta 1607*, 1−4.
29. Schägger, H., and von Jagow, G. (1987) Tricine-sodium dodecyl sulfate-polyacrylamide gel electrophoresis for the separation of proteins in the range from 1 to 100 kDa, *Anal. Biochem. 166*, 368−379.
30. Shevchenko, A., Wilm, M., Vorm, O., and Mann, M. (1996) Mass spectrometric sequencing of proteins from silver stained polyacrylamide gels, *Anal. Chem. 68*, 850−858.
31. Harauz, G., Boekema, E. J., and van Heel, M. (1988) Statistical image analysis of electron micrographs of ribosomal subunits, *Methods Enzymol. 164*, 35−49.
32. Penczek, P., Radermacher, M., and Frank, J. (1992) Three-dimensional reconstruction of single particles embedded in ice, *Ultramicroscopy 40*, 33−53.
33. Karapetyan, N. V., Holzwarth, A. R., and Rögner, M. (1999) The photosystem I trimer of cyanobacteria: molecular organization, excitation dynamics and physiological significance, *FEBS Lett. 460*, 395−400.
34. Boekema, E. J., van Roon, H., Calkoen, F., Bassi, R., and Dekker, J. P. (1999) Multiple types of association of photosystem II and its light-harvesting antenna in partially solubilized photosystem II membranes, *Biochemistry 38*, 2233−2239.
35. Gobets, B., van Stokkum, I. H. M., Rögner, M., Kruip, J., Schlodder, E., Karapetyan, N. V., Dekker, J. P., and van Grondelle, R. (2001) Time-resolved fluorescence emission measurements of photosystem I particles of various cyanobacteria: A unified compartmental model, *Biophys. J. 81*, 407−424.
36. Ben-Shem, A., Frolow, F., and Nelson, N. (2003) Crystal structure of plant photosystem I, *Nature 426*, 630−635.
37. Liu, Z., Yan, H., Wang, K., Kuang, T., Zhang, J., Gui, L., An, X., and Chang, W. (2004) Crystal structure of spinach major light-harvesting complex at 2.72 Å resolution, *Nature 428*, 287−292.
38. Ruban, A. V., Wentworth, M., Yakushevska, A. E., Andersson, J., Lee, P. J., Keegstra, W., Dekker, J. P., Boekema, E. J., Jansson, S., and Horton, P. (2003) Plants lacking the main light-harvesting complex retain photosystem II macro-organization, *Nature 421*, 648−652.

BI048772L